

Quantum computation using weak nonlinearities: robustness against decoherence

Hyunseok Jeong*

Centre for Quantum Computer Technology, Department of Physics,
University of Queensland, St Lucia, Qld 4072, Australia

(Dated: November 18, 2018)

We investigate decoherence effects in the recently suggested quantum computation scheme using weak nonlinearities, strong probe coherent fields, detection and feedforward methods. It is shown that in the weak-nonlinearity-based quantum gates, decoherence in nonlinear media *can be made arbitrarily small* simply by using arbitrarily strong probe fields, if photon number resolving detection is used. On the contrary, we find that homodyne detection with feedforward is not appropriate for this scheme because in this case decoherence rapidly increases as the probe field gets larger.

PACS numbers: 03.67.Mn, 42.50.Dv, 03.67.Lx, 42.50.-p

I. INTRODUCTION

Decoherence [1] is one of the main obstacles to the observation of quantum phenomena and the realization of quantum information processing (QIP). Since it is impossible to perfectly isolate a quantum system from its environment, decoherence effects are more or less unavoidable. Long-term existence of a macroscopic quantum superposition [2] is hindered by the decoherence effects [1, 3]. Overcoming the destructive effects of decoherence is the central issue for the realization of a large scale quantum computation (QC). Quantum error correcting codes and entanglement purification protocols have been developed to overcome the destructive effects of decoherence [4].

Strong nonlinear effects in optical systems, on the other hand, could be very useful for the observation of quantum phenomena [5, 6, 7] and the implementation of optical QIP [8]. Since currently available nonlinearities are extremely weak, optical fields need to pass through long nonlinear media for observable realizations of quantum effects. This would cause the decoherence effects overwhelming so that no quantum effects can actually manifest.

Recently, the idea of using weak cross-Kerr nonlinearities combined with strong coherent fields has been developed by several different authors and applied to various applications [9, 10, 11, 12, 13, 14, 15, 16, 17, 18, 19]. The general idea of the weak-nonlinearity-based approach is that the weak strength of a nonlinearity can be compensated by using a strong probe coherent field, $|\alpha\rangle$, with a very large amplitude α . In particular, Nemoto and Munro suggested a QC scheme using weak nonlinearities and linear optics [14], which has been further developed by Munro *et al.* [15, 16]. They also pointed out [17] that the weak-nonlinearity-based QC [14, 15, 16] has merit over the linear optics QC based on Knill *et al.*'s proposal [20] for a large scale quantum computation. However, a rigorous investigation of decoherence effects is essential

to verify the validity of the weak-nonlinearity-based QC in a real experiment.

Very recently, it was shown [11] that a SCS generation scheme [21] combined with the weak-nonlinearity-based approach [9, 10, 11, 12, 13, 14] can *per se* overcome decoherence in the nonlinear medium, i.e., as the amplitude α becomes large, decoherence during the nonlinear interaction *decreases*. In the concluding remarks of Ref. [11], it was naively conjectured that the QC scheme [14, 15, 16, 17] could also overcome the decoherence effects in the same way. However, it is unclear whether the weak-nonlinearity-based QC can truly overcome decoherence during the nonlinear interactions in this way with different detection-feedforward strategies [14, 15, 16, 17].

In this paper, we investigate decoherence effects in the weak-nonlinearity-based QC with homodyne detection [14, 15, 17] and photon number resolving detection [16]. We show that as the initial amplitude of the probe coherent state gets larger, decoherence rapidly *increases* in the two-qubit parity gate with homodyne detection [13, 14, 15, 17]. On the contrary, we find that as the initial amplitude of the probe coherent state gets larger, decoherence *diminishes* in the two-qubit parity gate with photon number resolving detection [16]. In other words, decoherence can be made *arbitrarily small* in this type of gates simply by increasing the probe field amplitude. We explain that this is due to the difference of the geometric requirements in the phase space. Since the two-qubit parity gate is the key element in the weak-nonlinearity-based QC [14, 15, 16, 17], our result shows that the weak-nonlinearity-based QC can naturally overcome decoherence effects but photon number resolving detection is needed for such robustness to decoherence.

II. THE TWO-QUBIT PARITY GATE USING WEAK NONLINEARITIES

It was shown that in conjunction with a strong coherent field, two weak nonlinearities are sufficient to implement a parity gate that entangles two qubits as illustrated in Fig. 1 [13, 14]. The interaction Hamiltonian of the cross-Kerr nonlinearity between modes a and p

*Electronic address: jeong@physics.uq.edu.au

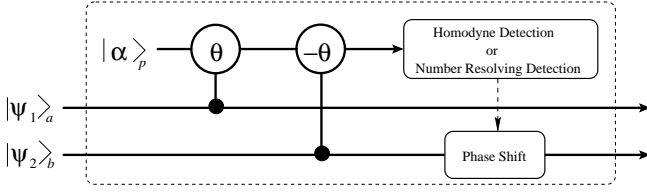


FIG. 1: A schematic of the parity gate using weak nonlinearities that entangles two qubits. The two-mode nonlinear interactions θ and $-\theta$ occur only for the horizontally polarized qubit state $|H\rangle$.

is $H_K = \hbar\chi\hat{a}_a^\dagger\hat{a}_a\hat{a}_p^\dagger\hat{a}_p$, where \hat{a} (\hat{a}^\dagger) represents the annihilation (creation) operator and χ is the nonlinear coupling constant. The interaction between a Fock state, $|n\rangle_a$, and a probe coherent state, $|\alpha\rangle_p$, is described as $U_K(t)|n\rangle_a|\alpha\rangle_p = |n\rangle_a|\alpha e^{i n \theta}\rangle_p$, where $\theta = \chi t$ with the interaction time t , and $U_K(t) = e^{i H_K/\hbar}$. Using polarization beam splitters, it is possible to use the horizontally and vertically polarized single-photon states, $|H\rangle$ and $|V\rangle$, to work as [14] $U_K(t)|H\rangle|\alpha\rangle = |H\rangle|\alpha e^{i\theta}\rangle$ and $U_K(t)|V\rangle|\alpha\rangle = |V\rangle|\alpha\rangle$. For simplicity, we assume two identical initial qubits, $|\Psi\rangle_a = (|H\rangle_a + |V\rangle_a)/\sqrt{2}$ and $|\Psi\rangle_b = (|H\rangle_b + |V\rangle_b)/\sqrt{2}$. The total initial state is

$$|\psi_i\rangle = \frac{1}{2}(|H\rangle + |V\rangle)_a(|H\rangle + |V\rangle)_b|\alpha\rangle_p \quad (1)$$

where α is assumed to be real without losing generality. After the first nonlinear interaction between modes a and p with angle θ , the initial state evolves to $|\psi_1\rangle = \{(|HH\rangle + |HV\rangle)_{ab}|\alpha e^{i\theta}\rangle_p + (|VH\rangle + |VV\rangle)_{ab}|\alpha\rangle_p\}/2$. After the second nonlinear interaction between modes b and p with angle $-\theta$, it becomes

$$|\psi_2\rangle = \frac{1}{2}\{(|HH\rangle + |VV\rangle)_{ab}|\alpha\rangle_p + |HV\rangle_{ab}|\alpha e^{i\theta}\rangle_p + |VH\rangle_{ab}|\alpha e^{-i\theta}\rangle_p\}. \quad (2)$$

A measurement is then performed to distinguish the probe beam $|\alpha\rangle_p$ from $|\alpha e^{i\theta}\rangle_p$ and $|\alpha e^{-i\theta}\rangle_p$, while it does not distinguish $|\alpha e^{i\theta}\rangle_p$ and $|\alpha e^{-i\theta}\rangle_p$.

Suppose that homodyne detection for quadrature $\hat{X} = (a + a^\dagger)/2$ is performed with the measurement result X . As can be seen in Fig. 2(a), the distinguishability of the measurement is determined by the distance

$$d_{HD} = \alpha(1 - \cos \theta) \approx \frac{\alpha\theta^2}{2} \quad (3)$$

where the approximation has been made under the assumptions of $\theta \ll 1$. Munro *et al.* pointed out that the error probability is $P_{err} \approx 10^{-4}$ for $d_{HD} = 4$ [15]. If d_{HD} is large enough and the measurement outcome is $X > X_{mid}$, where $X_{mid} = \alpha(1 + \cos \theta)/2$, the output state is

$$|\psi_f\rangle = \frac{1}{\sqrt{2}}(|HH\rangle + |VV\rangle)_{ab}. \quad (4)$$

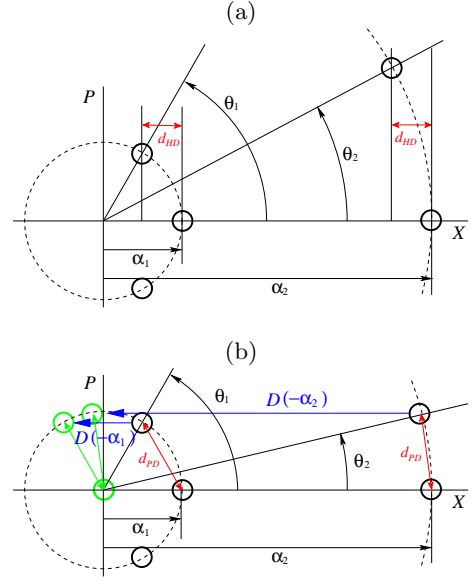


FIG. 2: Geometric diagram for the weak-nonlinearity-based two-qubit parity gate using (a) homodyne detection and (b) photon number resolving detection. (a) As the initial amplitude becomes large, the “travel path”, $\alpha\theta$, of the coherent state in the phase space should increase to maintain the distance d_{HD} , i.e., $\alpha_2\theta_2 > \alpha_1\theta_1$. This causes the increase of decoherence effects for large amplitudes. (b) Regardless of the initial amplitude, the travel path, $\alpha\theta$, of the coherent state of the same order can maintain the distance d_{PD} , i.e., $\alpha_2\theta_2 \approx \alpha_1\theta_1$. This reduces the decoherence effects because the interaction time t in a nonlinear medium becomes shorter as the initial amplitude increases.

On the other hand, if $X < X_{mid}$, the output state is $|\psi'_f\rangle = (e^{i\phi(X)}|HV\rangle + e^{-i\phi(X)}|VH\rangle)_{ab}/\sqrt{2}$, where $\phi(X) = 2\alpha \sin \theta (X - \alpha \cos \theta)$. One can transform the state $|\psi'_f\rangle$ to the state $|\psi_f\rangle$ by a simple phase shift for mode b [14, 15] based upon the measurement result.

Instead of homodyne detection, the photon number resolving detection can be used to distinguish the coherent state elements for mode p as shown in Fig. 2(b). [16]. The displacement operation $D(-\alpha)$ is then applied before photon number detection is performed. After the displacement operation, the state $|0\rangle$ can be distinguished from $|\alpha(e^{\pm\theta} - 1)\rangle$ by photon number resolving detection with measurement n_p . The output state (4) is obtained for $n_p = 0$. The resulting state for $n_p \neq 0$, $(e^{i\phi(n_p)}|HV\rangle + e^{-i\phi(n_p)}|VH\rangle)_{ab}/\sqrt{2}$, can be transformed to the state (4) by a phase shift with the phase factor $\phi(n_p) = n_p \tan^{-1}[\cot(\theta/2)]$. The distance d_{PD} which determines the distinguishability of the measurement is

$$d_{PD} = 2\alpha \sin \frac{\theta}{2} \approx \alpha\theta \quad (5)$$

and the error probability is $P_{err} \approx 10^{-4}$ for $d_{PD} = \pi$ [16].

III. DECOHERENCE IN THE WEAK-NONLINEARITY-BASED PARITY GATE

The ideal output state of the two-qubit parity gate should be the pure entangled state (4). However, the actual outcome state will be in a mixed state due to the decoherence effects *in the nonlinear media*. Photon losses may occur both in the probe field mode (p) and in the qubit modes (a and b). However, the possibility of losing photons in the qubit modes becomes lower as the initial amplitude gets larger, because the interaction times ($t = \theta/\chi$) in the nonlinear media become shorter as can be shown from Eqs. (3) and (5). The important factor of decoherence in the two-qubit output state (4) is photon losses in the probe field mode. Since the coherent field contains a large number of photons, it is easy to lose photons even in a very short time. Such photon losses in the probe coherent field cause the loss of phase information in the two-qubit output state (4). In particular, it is known that a superposition of two distant coherent states rapidly loses its coherence even when it loses a small number of photons [3]. Therefore, photon losses of the probe coherent field in the nonlinear media should be considered the main source of decoherence in the two-qubit output state. In what follows, we shall consider photon losses in the probe field and decoherence effects in the two-qubit output state caused by such photon losses.

Suppose that the probe coherent field loses photons in the first nonlinear medium as $|\alpha\rangle \rightarrow |\mathcal{A}\alpha\rangle$, where we define the amplitude parameter \mathcal{A} (≤ 1). After the first nonlinear interaction, the total initial state becomes a mixed state as

$$\begin{aligned} & \frac{1}{4} \left\{ (|HH\rangle + |HV\rangle)(\langle HH| + \langle HV|) \otimes |\mathcal{A}\alpha e^{i\theta}\rangle\langle \mathcal{A}\alpha e^{i\theta}| \right. \\ & + \mathcal{C}(|HH\rangle + |HV\rangle)(\langle VH| + \langle VV|) \otimes |\mathcal{A}\alpha e^{i\theta}\rangle\langle \mathcal{A}\alpha| \\ & + \mathcal{C}^*(|VH\rangle + |VV\rangle)(\langle HH| + \langle HV|) \otimes |\mathcal{A}\alpha\rangle\langle \mathcal{A}\alpha e^{i\theta}| \\ & \left. + (|VH\rangle + |VV\rangle)(\langle VH| + \langle VV|) \otimes |\mathcal{A}\alpha\rangle\langle \mathcal{A}\alpha| \right\}_{abp} \quad (6) \end{aligned}$$

where the coherent parameter, \mathcal{C} , is introduced to quantify the degree of dephasing. It is easy to recognize that *both* \mathcal{A} and \mathcal{C} should be reasonably large for the two-qubit parity gate to work properly at the end. If \mathcal{A} is large but \mathcal{C} is negligible, the final output state of the parity gate will be $\rho_f^{(m)} = (|HH\rangle\langle HH| + |VV\rangle\langle VV|)_{ab}/2$, which was also pointed out in Ref. [16]. This completely dephased state, $\rho_f^{(m)}$, does not contain entanglement, i.e., the two-qubit parity gate completely fails. On the other hand, if \mathcal{C} is close to 1 but \mathcal{A} is negligible, the final result will be $|\phi_f\rangle = (|H\rangle + |V\rangle)_a (|H\rangle + |V\rangle)_b/2$, which is simply identical to the unentangled initial qubits so that the gate also fails.

The decoherence effects for a state described by the density operator ρ can be induced by solving the master

equation [22]

$$\frac{\partial \rho}{\partial t} = \hat{J}\rho + \hat{L}\rho; \quad \hat{J}\rho = \gamma a \rho a^\dagger, \quad \hat{L}\rho = -\frac{\gamma}{2}(a^\dagger a \rho + \rho a^\dagger a) \quad (7)$$

where γ is the energy decay rate. The formal solution of the master equation (7) can be written as $\rho(t) = \exp[(\hat{J} + \hat{L})t]\rho(0)$ where t is the interaction time. The evolution of the initial density element $|\alpha\rangle\langle\beta|$ by the decoherence process $\tilde{\mathcal{D}}$ can be described as [22]

$$\tilde{\mathcal{D}}(|\alpha\rangle\langle\beta|) = e^{-\frac{1}{2}(1-e^{-\gamma t})\{(|\alpha|^2+|\beta|^2)+\alpha\beta^*\}} |\mathcal{A}\alpha\rangle\langle\mathcal{A}\beta|, \quad (8)$$

where $|\beta\rangle$ ($|\alpha\rangle$) is a coherent state with amplitude β (α) and $\mathcal{A} = e^{-\gamma t/2}$. However, it should be noted that the decoherence process ($\tilde{\mathcal{D}}$) occurs *simultaneously* with the unitary evolution ($\tilde{\mathcal{U}}$) by the cross-Kerr interaction Hamiltonian H_K in a nonlinear medium. This combined process can be modeled as follows [11]. One may assume that $\tilde{\mathcal{U}}$ occurs for a short time Δt , and then $\tilde{\mathcal{D}}$ occurs for another Δt . In other words, $\tilde{\mathcal{U}}$ and $\tilde{\mathcal{D}}$ continuously take turn for such short intervals in the nonlinear medium. By taking Δt arbitrarily small, one can obtain an extremely good approximation of this process for a given time t ($= N\Delta t$) with large integer number N . Let us set $\Delta\theta = \chi\Delta t = \pi/N$. In our calculation, we have chosen $N = 10^6$, i.e., $\Delta\theta = \pi/10^6$. This value gives a very good approximation for the whole range of α in our study [11]. Using this model, let us first consider the evolution of one cross term, $(|HH\rangle\langle VH|)_{ab} \otimes (|\alpha\rangle\langle\alpha|)_p$, in the initial state (1). After time t ($= N\Delta t$) in the nonlinear medium, it evolves to

$$\begin{aligned} & \left\{ \tilde{\mathcal{D}}_p(\Delta t) \tilde{\mathcal{U}}_{ap}(\Delta t) \right\}^N (|HH\rangle\langle VH|)_{ab} \otimes (|\alpha\rangle\langle\alpha|)_p \\ & = \mathcal{C}(|HH\rangle\langle VH|)_{ab} \otimes (|\mathcal{A}\alpha e^{i\theta}\rangle\langle \mathcal{A}\alpha|)_p \quad (9) \end{aligned}$$

where $\tilde{\mathcal{U}}(\Delta t)\rho \equiv U_K(\Delta t)\rho U_K^\dagger(\Delta t)$ and

$$\begin{aligned} \mathcal{C} &= \exp \left[-\alpha^2(1 - e^{-\gamma(t/N)}) \right. \\ & \left. \sum_{n=1}^N \exp[-\gamma(t/N)]^{(n-1)} (1 - \exp[-i\chi n(t/N)]) \right]. \quad (10) \end{aligned}$$

The amplitude parameter \mathcal{A} and the coherence parameter \mathcal{C} can then be obtained for an initial amplitude α . We shall use the absolute value of the coherence parameter $|\mathcal{C}|$ to assess the degree of dephasing.

We are interested in \mathcal{A} and $|\mathcal{C}|$ under experimentally realistic assumptions. It has been known that an optical fiber of about 3,000km may be required for a nonlinear interaction of $\theta = \pi$ using a currently available cross Kerr nonlinearity [23]. We first choose $\chi/\gamma = 0.0125$ that the amplitude will reduce as $\mathcal{A} \approx 0.533$ for 15km while $\theta = \pi$ is obtained for 3,000km. This corresponds 0.364dB/km of signal loss, which is a typical value for commercial fibers used for telecommunication and easily achieved using current technology [24, 25]. Note that signal losses in some pure silica core fibers are even less than

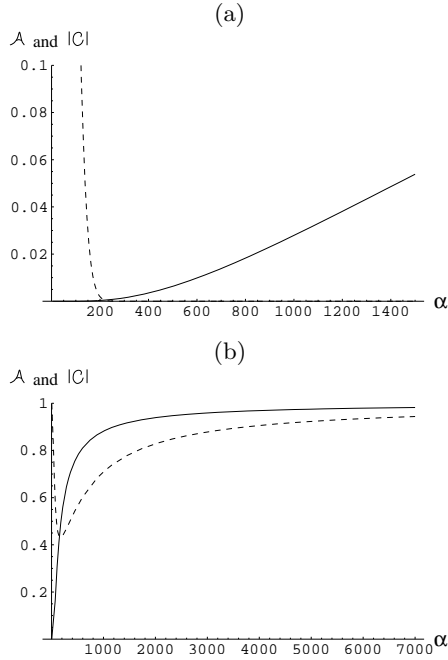


FIG. 3: The amplitude parameter \mathcal{A} (solid line) and the absolute coherence parameter $|\mathcal{C}|$ (dashed line) against the initial amplitude α for homodyne detection and photon number detection. The two-qubit parity gate works when both \mathcal{A} and $|\mathcal{C}|$ are large. (a) When homodyne detection is used: it is obvious that the condition of both \mathcal{A} and $|\mathcal{C}|$ being large cannot be met. (b) When photon number resolving detection is used: the condition is satisfied for a large α .

0.15dB/km [25]. The Fig. 3(a) shows that as the initial amplitude α increases for a fixed $d_{HD}(=4)$, the absolute coherence parameter $|\mathcal{C}|$ (dashed line) rapidly decreases for the homodyne detection scheme. The absolute coherence parameter $|\mathcal{C}|$ is not negligible only when α is small. However, the two-qubit parity gate does not work in this regime because \mathcal{A} (solid line) becomes extremely small. This means the probe coherent state becomes the pure vacuum so that a large $|\mathcal{C}|$ is meaningless. The Fig. 3(b) shows that this scheme with photon number detection does not suffer such problems: as the initial amplitude α increases for a fixed $d_{PD}(=\pi)$, both \mathcal{A} and $|\mathcal{C}|$ increases for large α . Some detailed values for $\chi/\gamma = 0.0125$ (0.364dB/km) and $\chi/\gamma = 0.0303$ (0.15dB/km) including the required length of optical fibers have been presented in Table I.

One can understand the difference between Fig. 3(a) and Fig. 3(b) by a simple geometric analysis in Fig. 2. For the case of homodyne detection, as the initial amplitude α gets larger, the “travel path” of the coherent state in the phase space, $\alpha\theta$, increases. (Even though θ decreases, the increase of α makes $\alpha\theta$ larger for a fixed $d_{HD}(\approx \alpha\theta^2/2)$ as shown in Fig. 2(a).) Therefore, the initial coherent state should travel longer in the phase space. This makes decoherence actually increase as α gets larger. In this case, the principle of increasing α to compensate small θ will not work efficiently. However,

TABLE I: The amplitude parameter \mathcal{A} and coherence parameter $|\mathcal{C}|$ under various conditions. α is the initial amplitude of the probe coherent state and ‘Length’ is the required length of the optical fiber. (a) Cases for homodyne detection with $d_{HD}(\approx \alpha\theta^2/2) = 4$. Comparing \mathcal{A} and $|\mathcal{C}|$, it is obvious that this detection strategy cannot be used for the weak-nonlinearity-based two-qubit parity gate. (b) Cases for photon number resolving detection with $d_{PD}(\approx \alpha\theta) = \pi$. Both \mathcal{A} and $|\mathcal{C}|$ approach 1 simultaneously when α becomes large.

(a) Homodyne detection					
χ/γ	$\theta(=\chi t)$	α	Length (km)	\mathcal{A}	$ \mathcal{C} $
0.0125	0.284	100	271	10^{-5}	0.210
	0.163	300	130	0.0014	~ 0
	0.052	3000	50	0.127	~ 0
0.0303	0.284	100	271	0.009	10^{-4}
	0.163	300	130	0.067	~ 0
	0.052	3000	50	0.427	~ 0
(b) Photon number resolving detection					
χ/γ	$\theta(=\chi t)$	α	Length (km)	\mathcal{A}	$ \mathcal{C} $
0.0125	0.0105	300	10	0.658	0.474
	1.05×10^{-3}	3000	1	0.959	0.878
	1.05×10^{-4}	3×10^4	0.1	0.996	0.985
0.0303	0.0105	300	10	0.841	0.644
	1.05×10^{-3}	3000	1	0.983	0.946
	1.05×10^{-4}	3×10^4	0.1	0.998	> 0.99

the mechanism is totally different when photon number resolving detection is used. As the initial amplitude α gets larger, the travel path $\alpha\theta$ does not increase for a fixed $d_{PD}(\approx \alpha\theta)$ but remains approximately the same (see Fig. 2(b)). Therefore, the coherent state travels the same distance regardless of α , while the interaction time $t(=\theta/\chi)$ depending on θ keep decreasing as α increases. Such decrease of the interaction time t for the same distance causes the decrease of decoherence.

IV. REMARKS

In the weak-nonlinearity-based QC scheme, a strong probe coherent field with a large amplitude is necessarily required. However, as the amplitude of the coherent field gets larger, decoherence during a nonlinear interaction rapidly *increases* when homodyne detection is used. On the contrary, decoherence *diminishes* under the same condition when the photon number resolving measurement is used. This shows that the weak-nonlinearity-based QC can naturally overcome decoherence during the nonlinear interactions simply by using strong probe fields, when photon number resolving detection is used.

Since $d_{PD} = \pi$ in Eq. (5) is required for a small error probability, the photodetector for the two-qubit gate should be able to discriminate about 10 ($\approx d_{PD}^2$) photons. Such detection ability is extremely demanding using current technology. It may be crucial to first de-

velop the photon number resolving QND technique using a weak nonlinearity, a strong coherent field and homodyne detection in Ref. [12], which was employed for the two qubit gate in Ref. [16]. Here, we point out that the QND technique in Ref. [12] does *not* suffer the increase of decoherence for large probe field amplitudes in the nonlinear medium because distinguishability of this QND scheme [12] depends on $\approx \alpha\theta$, not on $\approx \alpha\theta^2$.

Using photon number resolving detection in the weak-nonlinearity-based two-qubit parity gate also requires a highly precise displacement operation, $D(-\alpha)$, with a very large α . The displacement operation can be performed using a strong coherent field and a beam splitter with high transmittivity. It would be experimentally challenging since the average photon number of the probe coherent field should be $|\mathcal{A}^2\alpha|^2 \gg 10^6$ to obtain good coherence as can be seen in Table I(b).

The two-qubit parity gate which we have considered in

this paper is based on two weak nonlinearities, a probe coherent field, a probe beam measurement and classical feedforward as shown in Fig. 1 [14, 15, 16, 17]. Here, we finally note the recently suggested weak-nonlinearity-based controlled-phase gate by Spiller *et al.* [26], where the probe beam measurement is not necessary at the cost of using additional nonlinearities and displacement operations. The requirement of successful achievement of this gate is $\alpha\theta \sim 1$ [26, 27], which satisfies the condition for the robustness against decoherence analyzed in this paper. Therefore, such an approach without the probe beam measurement may be considered as an alternative of the weak-nonlinearity-based parity gate in Fig. 1 using photon number resolving detection.

This work was supported by the Australian Research Council. The author would like to thank S.D. Barrett, T.C. Ralph, A.M. Branczyk and W.J. Munro for valuable comments and stimulating discussions.

-
- [1] W.H. Zurek, *Physics Today* **44**, 36 (1991).
 - [2] E. Schrödinger, *Naturwissenschaften*. **23**, 807-812; 823-828; 844-849 (1935).
 - [3] M. S. Kim and V. Bužek, *Phys. Rev. A* **46**, 4239 (1992).
 - [4] C. H. Bennett, D. P. DiVincenzo, J. A. Smolin and W. K. Wootters, *Phys. Rev. A* **54**, 3824 (1996).
 - [5] B. Yurke and D. Stoler, *Phys. Rev. Lett.* **57**, 13 (1986).
 - [6] Q.A. Turchette, C.J. Hood, W. Lange, H. Mabuchi and H.J. Kimble, *Phys. Rev. Lett.* **75**, 4710 (1995).
 - [7] M. Brune, E. Hagley, J. Dreyer, X. Maitre, A. Maali, C. Wunderlich, J.M. Raimond, and S. Haroche, *Phys. Rev. Lett.* **77**, 4887 (1996).
 - [8] G. J. Milburn, *Phys. Rev. Lett.* **62**, 2124 (1989).
 - [9] J. Fiurášek, L. Mišta, Jr. and R. Filip, *Phys. Rev. A* **67**, 022304 (2003).
 - [10] H. Jeong, PhD thesis, Queen's University Belfast, UK (2003).
 - [11] H. Jeong, *Phys. Rev. A* **72**, 034305 (2005).
 - [12] W. J. Munro, Kae Nemoto, R. G. Beausoleil, and T. P. Spiller, *Phys. Rev. A* **71**, 033819 (2005).
 - [13] S. D. Barrett, P. Kok, K. Nemoto, R. G. Beausoleil, W. J. Munro, and T. P. Spiller, *Phys. Rev. A* **71**, 060302(R) (2005).
 - [14] K. Nemoto and W. J. Munro, *Phys. Rev. Lett.* **93**, 250502 (2004).
 - [15] W.J. Munro, Kae Nemoto, T.P. Spiller, S.D. Barrett, Pieter Kok, and R.G. Beausoleil, *J. Opt. B* **7**, S135 (2005).
 - [16] W. J. Munro, K. Nemoto and T. Spiller, *New J. Phys.* **7**, 137 (2005).
 - [17] *Phys. Lett. A*, **344**, 104 (2005).
 - [18] H. Jeong, M.S. Kim, T.C. Ralph, and B.S. Ham, *Phys. Rev. A* **70**, 061801(R) (2004).
 - [19] M.S. Kim and M. Paternostro, quant-ph/0510057.
 - [20] E. Knill, R. Laflamme and G. J. Milburn, *Nature* **409**, 46 (2001).
 - [21] C. C. Gerry, *Phys. Rev. A* **59**, 4095 (1999).
 - [22] S. J. D. Phoenix, *Phys. Rev. A* **41**, 5132 (1990).
 - [23] B. C. Sanders and G. J. Milburn, *Phys. Rev. A* **45**, 1919 (1992); *Phys. Rev. A* **39**, 694 (1989).
 - [24] H. Kanamori, H. Yokota, G. Tanaka, M. Watanabe, Y. Ishiguro, I. Yoshida, T. Kakii, S. Itoh, Y. Asano and S. Tanaka, *IEEE J. Lightwave Tech.* **4**, 1144 (1986); S.A. Bashar, *Proc. IEB 2nd Int'l Conf. on Electrical Engineering*, Oct. 23rd-24th, Khulna, Bangladesh (2002).
 - [25] K. Nagayama, M. Matsui, M. Kakui, T. Saitoh, K. Kawasaki, H. Takamizawa, Y. Ooga, I. Tsuchiya and Y. Chigusa, *SEI Tech. Rev.* **57**, 3 (2004).
 - [26] T. P. Spiller, Kae Nemoto, Samuel L. Braunstein, W. J. Munro, P. van Loock and G. J. Milburn, quant-ph/0509202.
 - [27] W.J. Munro, private communication.